



## OPEN ACCESS

## EDITED BY

Liqun Yang,  
Shengjing Hospital of China Medical  
University, China

## REVIEWED BY

Bhupendra Gopalbhai Prajapati,  
Ganpat University, Gujarat, India  
Xuefang Hao,  
Inner Mongolia University for  
Nationalities, China

## \*CORRESPONDENCE

Guiyun Jin,  
✉ 13976609625@163.com  
Xueying Ji,  
✉ jixueying@163.com

†These authors have contributed equally  
to this work

RECEIVED 29 October 2023

ACCEPTED 11 December 2023

PUBLISHED 08 January 2024

## CITATION

Wei S, Deng T, Wu C, Shi J, Liao Y,  
Huang L, Liu Y, Zhong S, Ji X and Jin G  
(2024), Application of modified sodium  
alginate hydrogel for interventional  
embolization of hemorrhagic diseases.  
*Front. Mater.* 10:1329667.  
doi: 10.3389/fmats.2023.1329667

## COPYRIGHT

© 2024 Wei, Deng, Wu, Shi, Liao, Huang,  
Liu, Zhong, Ji and Jin. This is an  
open-access article distributed under  
the terms of the [Creative Commons  
Attribution License \(CC BY\)](https://creativecommons.org/licenses/by/4.0/). The use,  
distribution or reproduction in other  
forums is permitted, provided the  
original author(s) and the copyright  
owner(s) are credited and that the  
original publication in this journal is  
cited, in accordance with accepted  
academic practice. No use, distribution  
or reproduction is permitted which does  
not comply with these terms.

# Application of modified sodium alginate hydrogel for interventional embolization of hemorrhagic diseases

Shengchao Wei<sup>1,2,3†</sup>, Tang Deng<sup>4†</sup>, Caixia Wu<sup>3,5†</sup>, Jianshan Shi<sup>1</sup>,  
Yong Liao<sup>1</sup>, Lin Huang<sup>4</sup>, Yongjie Liu<sup>3,5</sup>, Shijie Zhong<sup>1</sup>,  
Xueying Ji<sup>5\*</sup> and Guiyun Jin<sup>1,2,3\*</sup>

<sup>1</sup>Department of Interventional Radiology and Vascular Surgery, The First Affiliated Hospital of Hainan Medical University, Hainan Medical University, Haikou, China, <sup>2</sup>Department of Emergency, The First Affiliated Hospital of Hainan Medical University, Hainan Medical University, Haikou, China, <sup>3</sup>Key Laboratory of Emergency and Trauma of Hainan Medical University, Ministry of Education, Key Laboratory of Hainan Trauma and Disaster Rescue, Hainan Medical University, Haikou, China, <sup>4</sup>Division of Vascular Surgery, The First Affiliated Hospital, Sun Yat-sen University, Guangzhou, China, <sup>5</sup>Hainan Medical University, Haikou, China

Traditional particulate embolic agents are small in diameter, but can easily embolize the ends of blood vessels, resulting in ischemia and necrosis of normal tissues and organs. The metal spring embolic agent has a larger diameter, but it cannot be degraded and can easily cause permanent damage to blood vessels. Ideally, a bleeding embolism should achieve rapid hemostasis without causing long-term necrosis of organs and tissues. In this study, a modified sodium alginate hydrogel (MSAH) was prepared by mixing an oxidized sodium alginate (OSA) aqueous solution with a carboxymethyl chitosan (CMC) aqueous solution at a ratio of 1:6 in a 38°C bath for 8 min. The feasibility of this modified hydrogel was then tested in an internal iliac artery hemorrhage model using New Zealand rabbits. The MSAH had good adhesion. The hydrogel was injected through a single curved 4F catheter without obvious effects on uterine smooth muscle cell proliferation and apoptosis. The blood flow of the internal iliac artery was restored by long-term degradation of the sodium alginate hydrogel, and no ischemia and necrosis were observed by histopathology. The MSAH prepared using a mixture of OSA and CMC had good adhesion, biocompatibility, and injectability and could be used for target-vessel embolization in an internal iliac artery hemorrhage model. The MSAH can achieve main artery embolization without affecting the peripheral artery blood supply, resulting in both short-term rapid hemostasis and long-term degradation, with no target organ necrosis.

## KEYWORDS

modified sodium alginate hydrogel, embolic agent, animal model of hemorrhage, interventional embolization, biomaterial

## Introduction

Hemorrhagic diseases, including pelvic fracture bleeding, postpartum hemorrhage (PPH), and acute upper gastrointestinal bleeding (AUGIB), are commonly seen in emergency departments, accounting for approximately 15%–20% of emergent visits every year (Majeed et al., 2016). Pelvic fractures account for about 3% of all fractures

(Chen et al., 2017) and are the main cause of death within 24 h after injury due to massive bleeding, with a fatality rate of as high as 40% (Cothren et al., 2007). In addition, the proportion of pregnant and lying-in women aged over 35 years was as high as 17.13% nationwide, and 53.9% of maternal deaths were directly due to obstetric causes, with PPH being the number one cause of maternal death (Butwick et al., 2020; Liu and Lei, 2020; Zaidi et al., 2020). Furthermore, in the United States, more than 400,000 patients have been hospitalized every year because of AUGIB, with an annual death toll of more than 30,000 people (Cappell and Friedel, 2008).

Early and rapid hemostasis, including drug hemostasis, surgery, and interventional therapy, is critical for the treatment of hemorrhagic diseases. Interventional hemostatic therapy achieves the goal of hemostasis by identifying the bleeding vessel using digital subtraction angiography (DSA) and blocking the blood flow using embolic materials. Interventional therapy has become the first choice for the treatment of fatal bleeding diseases due to several advantages such as accuracy, rapidity, minimal invasion, no absolute contraindication, and repeatability. Ideally, a bleeding embolism should achieve rapid hemostasis without long-term necrosis of the tissues and organs. At present, the commonly used endovascular embolic materials include gelatin sponge particles (Alicon), alginate microspheres (SHENGYIYAO), polyvinyl alcohol (Merit), and metal coils (COOK, Boston). Traditional particulate embolic agents have a diameter of 100–2,000  $\mu\text{m}$ , but these can block the vascular ends and cause ischemia and necrosis of normal tissues and organs. Although metal coils have a relatively large diameter and can block the vascular trunks, they cannot be degraded, and thus can easily cause permanent damage to blood vessels.

Oxidized sodium alginate (OSA) has been widely prepared as a biomedical material due to its swelling, extensibility, biocompatibility, adhesion, and biodegradability. Chen et al. planted rabbit bone marrow mesenchymal stem cells on SA hydrogel scaffolds, and the mesenchymal stem cells demonstrated survival after 1, 3, 5, and 7 days of culture on the scaffolds. On day 7, the cells proliferated rapidly on the scaffolds, and the cells exhibited a spindle shape, indicating that the mesenchymal stem cells not only survived on the scaffolds but could proliferate and differentiate normally. Thus, the alginate hydrogel scaffolds showed good biocompatibility. Mineralized alginate microspheres (M-ALG) have good biocompatibility and osteogenic properties (Chen et al., 2018). To verify the degradability of OSA, Park et al. conducted two cartilage regeneration studies on alginate and OSA. They preferentially mixed unoxidized SA with hyaluronic acid and injected this mixture with calcium to form a physical hydrogel for cartilage regeneration. They found that the non-oxidized alginate hydrogel remained in the animal model after cartilage regeneration, but under the same conditions, the oxidized alginate hydrogel treated with alginate completely degraded within 60 days (Park and Lee, 2014). Zhao et al. loaded SA hydrogel microspheres onto chondrocytes of New Zealand rabbits to study the degradation of the SA hydrogel microspheres. They found that the degradation time of the SA hydrogel *in vivo* and *in vitro* was 1 week and 4 weeks, respectively, and the complete degradation time was 4 and 6 weeks, respectively (Yu et al., 2016). In addition, Wu et al. subcutaneously implanted the SA hydrogel scaffold seeded with Schwann cells in the backs of rats, and showed that some of the alginate

hydrogel scaffolds were degraded 4 weeks later (Wu et al., 2020). Devi et al. prepared calcium ion crosslinked alginate composite microspheres as bone graft substitutes (Yashaswini et al., 2021; Liu et al., 2023).

OSA is often used to prepare SA microspheres. The alginate microsphere is commonly used in embolization treatment of benign and malignant tumors and achieves the therapeutic goal of causing tumor necrosis. However, when used for the treatment of hemorrhagic diseases, due to its small diameter, it can embolize the ends of blood vessels and cause ischemia and necrosis of normal tissues and organs (Tada et al., 2007). In this study, we prepared a modified SA hydrogel by mixing an OSA aqueous solution with a carboxymethyl chitosan (CMC) aqueous solution. The modified hydrogel retains the advantages of SA, such as biocompatibility, non-toxicity, and degradability, but also possesses new characteristics such as high strength and strong viscosity. Because the hydrogel does not embolize the terminal branch of the bleeding artery and can be degraded, it cannot cause long-term ischemia and necrosis of organs and is expected to become a new and safe embolic material for clinical application.

## Materials and methods

### Instruments and materials

The instruments and materials used in this study include biomicroscope (Laika, Germany), analytical balance (Seidolis), collector magnetic agitator (Jintan Medical Instrument Factory), digital subtraction angiography (GE), SA (Shenyang Bramble), CMC (Shanghai Macklin), sodium periodate (Zhejiang Haichuan), ethanol (Xilong Science and Technology), 21 G needle (Cook, United States), V18 Guide Wire (Boston Scientific, United States), microcatheter micro guide wires (Boston Scientific, United States), iohexol injection (GE, United States), Semisynne II (Dunhua Santa), Choutet 50 (Vicker, France), GELFOAM particles (ALICON), and embolized coil (COOK, United States).

### Laboratory animals

New Zealand female rabbits (6 months old, weighing 8–10 kg) were purchased from Tian Qin, Changsha, China (permit no. SCXK (Hunan) 2019-0015). The animals were bred and treated according to the requirements for the management of experimental animals.

### Preparation of MSAH

A dispersion of SA in ethanol was prepared by dissolving 10 g of SA in 50 g of ethanol using an analytical balance and stirring for 2 h using a magnetic agitator heated by a collector. NAI04 was dissolved in 50 mL of pure water, and the sodium periodate was dissolved in 50 mL of pure water. The mixture was mixed at room temperature in the ratio of N (NAIO4/SA) = 1 and then left to react in the dark for 4 h. After the oxidation reaction was completed, ethylene glycol with the same mass fraction as NAI04

was added, and the reaction was stopped for 30 min. SA was precipitated using ethanol with a volume ratio of 1:5, and the powder was obtained. After vacuum drying, the residual iodate and ethanol were removed using dialysis with distilled water for 3 days, and the OSA powder was obtained using lyophilization of the purified product.

OSA and CMC were mixed in a flask at ratios of 1:1, 1:2, 1:4, 1:6, 1:8, and 1:10, and shaken for 1 min. The mixture was placed in a 38°C bath for 1–9 min. The time for formation of the OSA aqueous solution and CMC aqueous solution was observed to obtain the fastest gelatinous ratio of the solution with the fastest gel formation time. To obtain the best gel formation time, the modified sodium alginate hydrogel (MSAH) was placed in the bath for 1–9 min and then injected onto glass slides with a 5-mL syringe to observe gel formation.

## Biocompatibility of the injectable MSAH

Uterine smooth muscle cells (USMCs) were cultured in a high glucose medium (Control group) and high glucose medium with the MSAH (MSAH group). The growth of the USMCs was observed at 3, 6, 12, 24, 48, and 72 h. After culturing for 72 h, the cell proliferation rate was detected using the CCK8 kit, and apoptosis rates were detected using flow cytometry.

## Injectability and adhesion of the MSAH

The MSAH was extracted with a 1-mL syringe and injected through a 4F single-curved catheter and a microcatheter, respectively. The injectability of the MSAH was evaluated by observing whether the MSAH was successfully injected on the glass slides through a 4F single curved catheter and microcatheter. The MSAH was injected into food-grade silica gel tubes with inner diameters of 16, 12, and 5 mm, respectively, and the adhesion to the tube wall was observed.

## Evaluating the effects of the MSAH in the animal hemorrhage model

Twenty New Zealand female rabbits (3 months old, weighing 8–10 kg) were randomly divided into four groups ( $n = 5$  for each group): Control group; MSAH group, embolized with MSAH; Gelfoam group, embolized with gelfoam particles; and Coil group, embolized with coil. The internal iliac artery (IIA) hemorrhage model was successfully established in the MSAH group, Gelfoam group, and Coil group, and the internal iliac arteries were embolized by injecting the MSAH, gelfoam particles, and coils via a microcatheter, respectively. Embolization was evaluated using angiography immediately after embolization. The puncture point of the left CCA was pressed with a gelatin sponge for 30 min until no blood overflow from the CAA was observed. The operation area was sterilized, and the skin was sutured and bandaged with sterile gauze. After waking from anesthesia, the rabbits were placed back in the experimental center, and penicillin (500,000 u/d) was administered

1 week after the operation to prevent infection. DSA was performed 1 month after the operation to check the recanalization of the bilateral internal iliac arteries.

## Assessment of plasma inflammatory factors

Blood (2 mL) was collected from the ear vein into a sterile centrifuge tube containing sodium citrate after the first angiography in the Control group, and 3 days after IIA embolization in the MSAH group, Gelfoam group, and Coil group. After centrifugation, the plasma was collected with a pipette and the precipitate was discarded. Plasma levels of tumor necrosis factor- $\alpha$  (TNF- $\alpha$ ) and interleukin (IL)-1 $\beta$  were determined using ELISA kits.

## Histopathology

The rabbits were euthanized by air embolism after the first angiography (Control group) or after bilateral IIA embolization (MSAH group, Gelfoam group, and Coil group). The uterus was removed to observe pathological changes in the uterine smooth muscle using hematoxylin and eosin (HE) staining.

## ELISA

The uterus was cut with scissors, and the tissue was homogenized in a glass homogenizer. After centrifugation at 4°C, the supernatant was obtained. The levels of tumor growth factor (TGF- $\beta$ ) and IL-1 $\beta$  in the tissue homogenates were detected using ELISA kits.

## Statistical analysis

SPSS25.0 statistical software was used to analyze the data. Data with normal distribution are expressed as mean and standard deviation and were analyzed using the independent sample *t*-test.  $p < 0.05$  was considered statistically significant.

## Results

### Preparation and performance evaluation of MSAH

The OSA aqueous solution and CMC aqueous solution at a ratio of 1:1 was largely ungelatinized. The mixtures at ratios of 1:2, 1:4, 1:6, 1:8, and 1:10 were gelatinized at 4 min and complete gelatinization was achieved at 15 min in a 38°C water bath (Figure 1A). The mixture at the ratio of 1:6 had the fastest gelatinization time, which exhibited gelatinization at 4 min and stabilized at 8 min (Figure 1B). A stable MSAH was prepared by placing the OSA aqueous solution and CMC aqueous solution at a ratio of 1:6 into a 38°C water bath for 8 min and was injected on the slide using a syringe, a glue-head

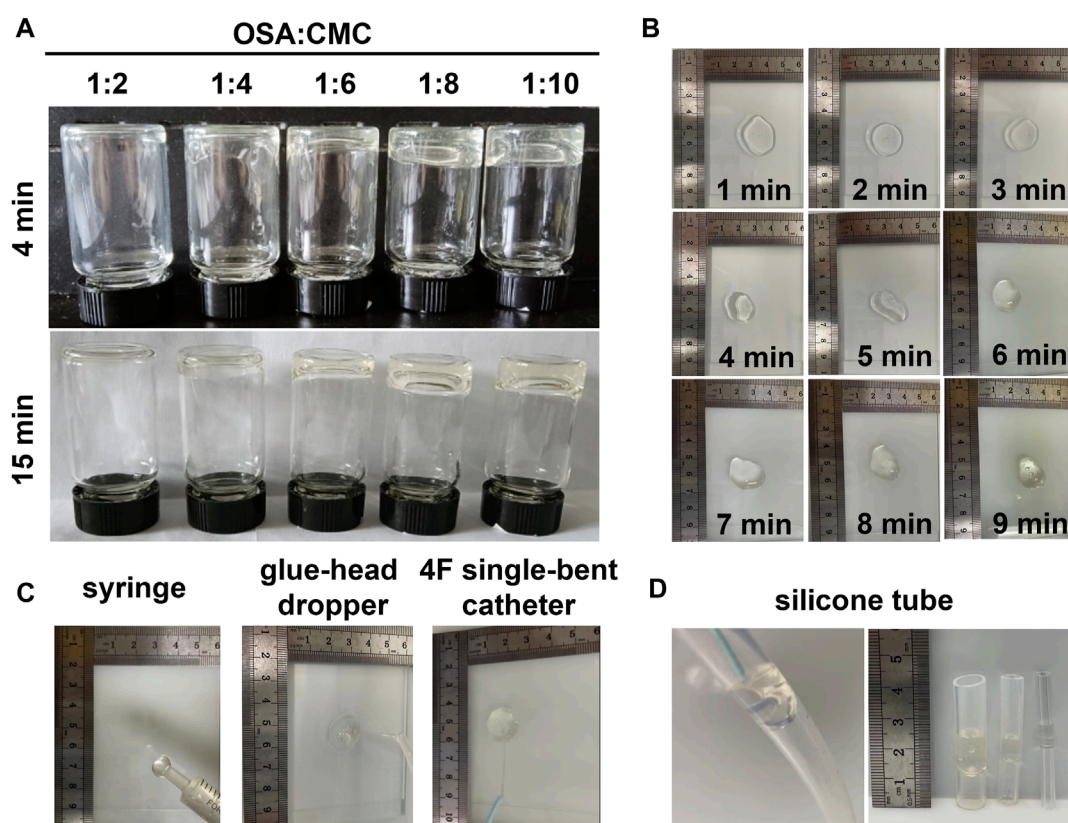


**FIGURE 1**

Preparation and evaluation of MSAH. **(A)** OSA aqueous solution: Gelling of CMC aqueous solution at different proportions; **(B)** gel formation of MSAH at different times in the water bath; **(C)** injectability of the MSAH was verified by using 1 mL syringe, 4F single curved catheter and microcatheter; **(D)** The MSAH was injected into food-grade silica gel tubes with inner diameters of 16mm, 12mm and 5 mm to verify its adhesion.

dropper, and a 4F single-bent catheter (Figure 1C). The hydrogel was injected into silicone tubes using a syringe through a 4F single-bent catheter and adhered to different diameters of silicone tube walls (Figure 1D).

USMCS WERE treated with MSAH for 72 h in the MSAH group (Figure 2A). There was no significant difference in the proliferation rate between the MSAH group and the Control group ( $p > 0.05$ ; Figure 2B), and there was no significant difference in the apoptosis rate between the MSAH group and the control group (Figures 2C–E).

## Establishment of the hemorrhage model

New Zealand female rabbits were fasted for 12 h before the operation. Anesthesia was induced by xylazine hydrochloride injection II (2 mg/kg) and maintained by intravenous injection of Zoletil (7.5 mg/kg). The left common carotid artery (CCA) was passively separated using elbow hemostatic forceps (12.5 cm) (Figure 3). After placement of 2–0 Mousse thread at the proximal and distal segments, the left CCA was punctured with a 21 g micropipette, and a V18-wire exchange microcatheter was inserted. Heparin saline (0.5 mg/kg) was infused into the artery according to the weight of rabbits.

Under the road map, the microcatheter was super-selected into the left internal iliac artery. After the microcatheter was fixed, the microcatheter was removed, and the hard end of the V18 guide wire was entered into the microcatheter to quickly puncture the left internal iliac artery. The leakage of contrast media in the left IIA was confirmed using angiography. Before and 10 min after the establishment of the IIA hemorrhage model, 5 mL of whole blood was taken from the ear vein and placed into the blood collection tube containing EDTA-k2 anticoagulants. Red blood cell (RBC) count, hemoglobin (HGB) content, and hematocrit (HCT) were measured using a hematology analyzer. No infection, death, hematuria, bloody stool, hemiplegia, lip deviation, or any other complications of cerebral infarction were found in any of the rabbits. In the first 3 days after modeling, the appetite and mental state of the rabbits decreased.

## DSA of the rabbit model

According to the angiographic findings, the vascular anatomy of the rabbit was similar to that of the human body. Angiographic results via subclavian artery catheterization showed that the brachiocephalic trunk (BCT), left CCA, left subclavian artery (LSA), and right subclavian artery (RSA) originated from the aortic arch.

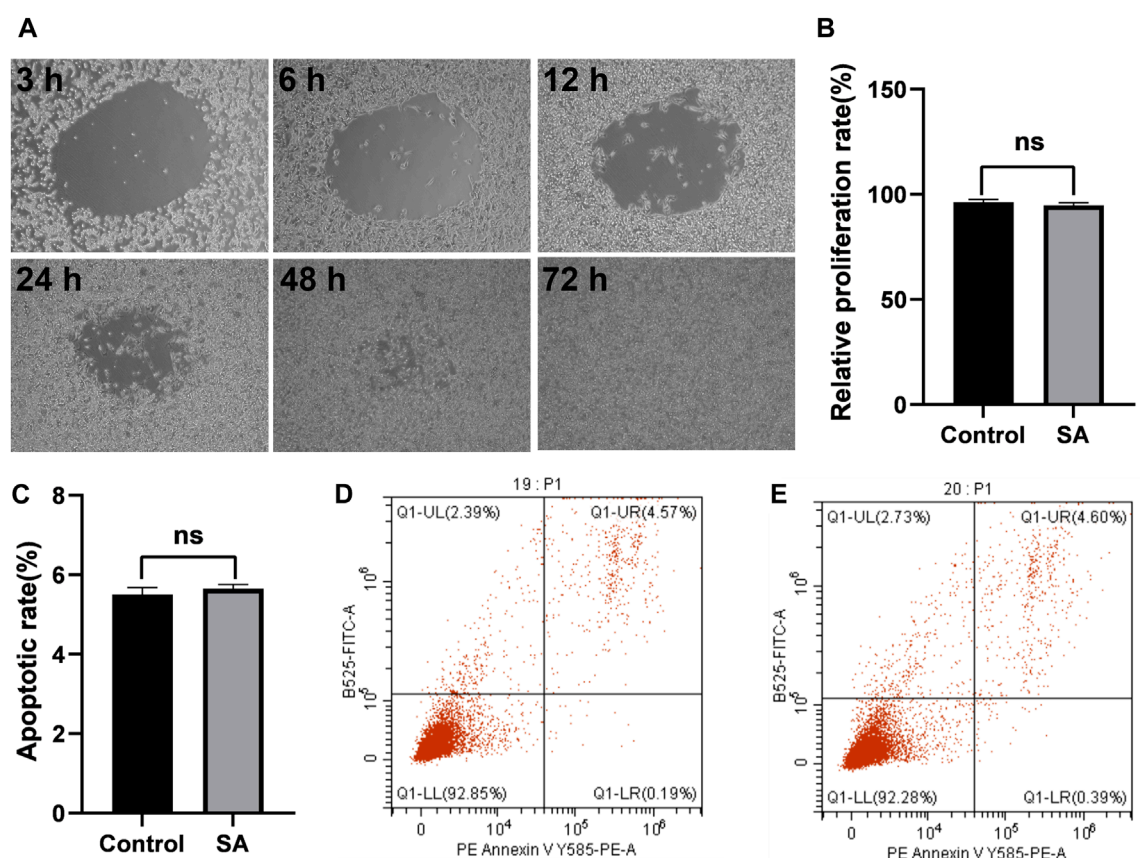


FIGURE 2

Cell compatibility of the MASH. (A) Proliferation of USMCs in the SA group at different times, (B) proliferation rate of USMCs in the MSAH group and Control group, (C) apoptosis rate of USMCs in the MSAH group and Control group, (D) apoptosis rate of USMCs in the Control group, and (E) apoptosis rate of USMCs in the MSAH group.

The celiac axis (CA), splenic artery (SA), superior mesenteric artery (SMA), left renal artery (LRA), and right renal artery (RRA) were visualized on the upper segment of the abdominal aorta, and the common iliac artery (CIA) was visualized on the lower segment of the abdominal aorta. The IIA was the first branch of the CIA, followed by the external iliac artery (EIA), common femoral artery (CFA), and deep femoral artery (DFA). The left IIA showed the superior gluteal artery (SGA), inferior gluteal artery (IGA), uterine artery (UA), vesical arteries (VA), and internal pudendal artery internal iliac artery (IPA) (Figure 4A).

## DSA images before and after establishing the hemorrhage model

Before establishing the hemorrhage model, the bilateral IIA showed normal deformation without abnormal stenosis and tumor-like dilatation. After the microcatheter was placed on the left IIA, the left IIA was punctured by the hard end of the V18 guide wire, and signs of hemorrhage were observed, evidenced by the spilling of the contrast medium. After the bilateral IIA was super-selected

separately via the microcatheter and embolized with a self-made gelatin sponge strip, DSA showed that the bilateral IIA was blocked, and bleeding signs disappeared (Figure 4B).

## Erythrocyte count, hemoglobin and hematocrit

Before establishing the hemorrhage model, total RBC was 4.4 d th12/L, HGB content was 93 G/L, and HCT was 32%. After model establishment, the total RBC was 3.6 days th12/L, HGB content was 75 G/L, and HCT was 25%. The levels of RBC (Figure 4C), HGB (Figure 4D), and HCT (Figure 4E) after model establishment were significantly lower than before model establishment ( $p < 0.01$ ).

## Effects of different embolic materials in the hemorrhage model

DSA images before establishing the hemorrhage model showed that the bilateral IIA and its branches were visualized in the MSAH

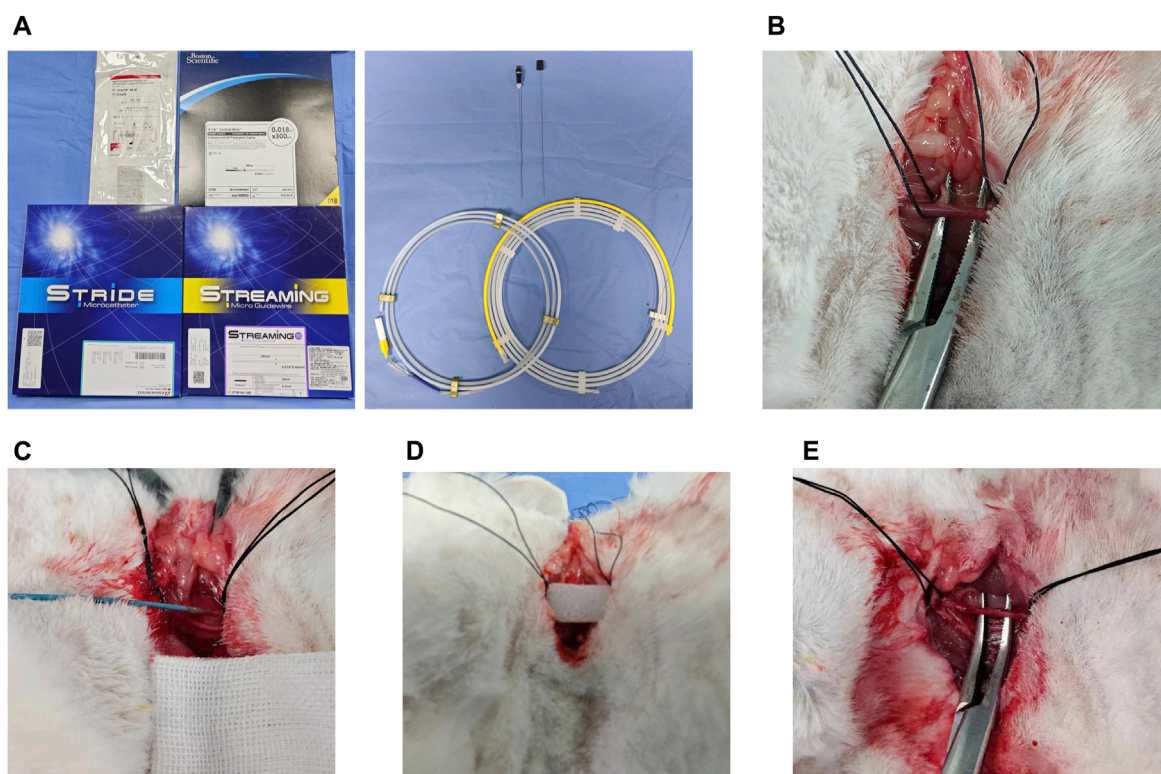


**FIGURE 3** Hemorrhagic rabbit model established using interventional therapy. (A) Surgical instrument; (B) leaky carotid artery; (C) microcatheter placement in the carotid artery; (D) postoperative gelfoam tablet compression puncture point; and (E) carotid artery healed postoperatively.

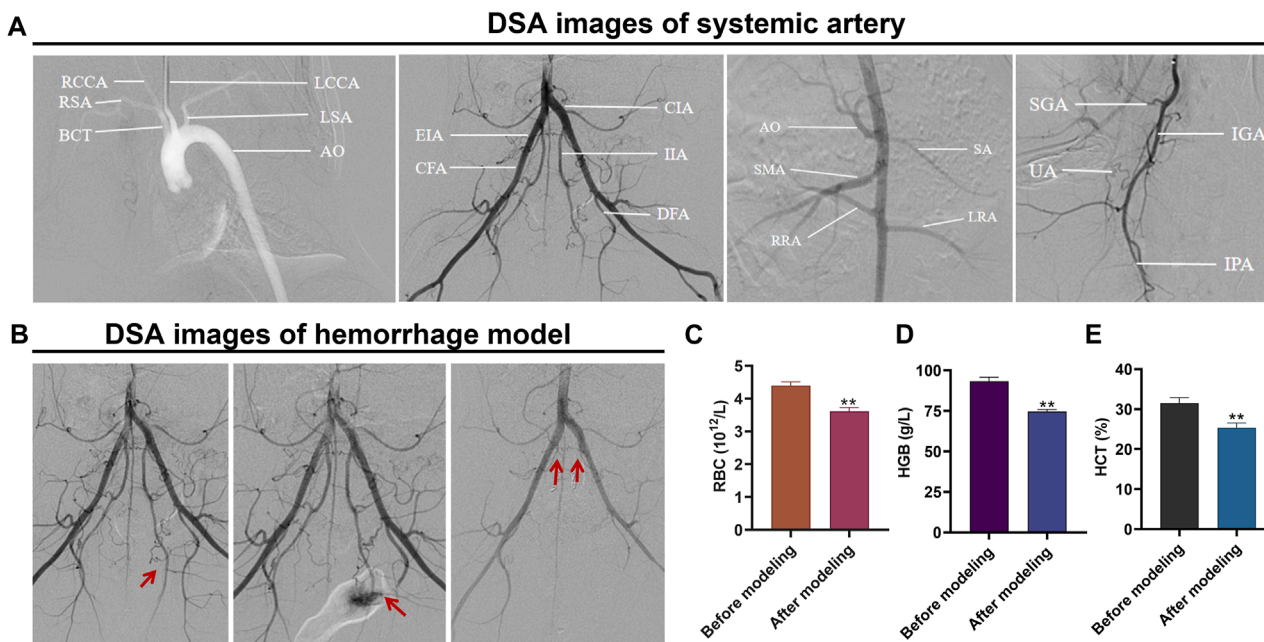


**FIGURE 4** Hemorrhagic rabbit model established using interventional therapy. (A) DSA image of the systemic artery; (B) DSA images of the hemorrhage model before and after establishment and embolization; (C) changes in RBC, HGB, and HCT levels before and after establishment of the hemorrhage model; (D) changes in HGB levels before and after establishment of the hemorrhage model; and (E) changes in HCT levels before and after establishment of the hemorrhage model.

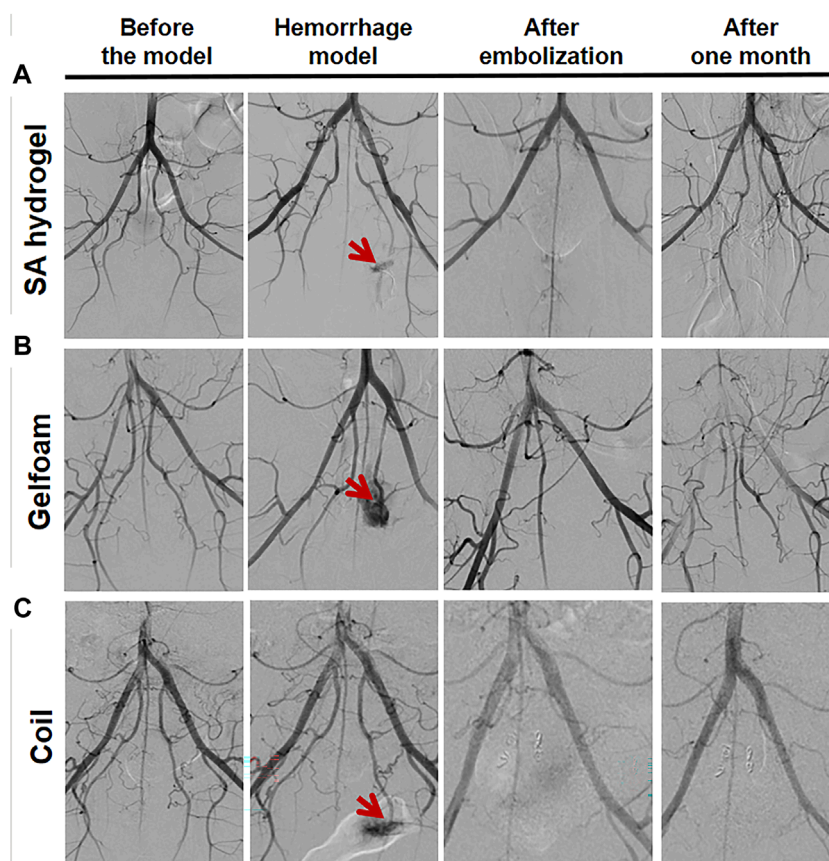


**FIGURE 5**

DSA images of IIA bleeding following embolization with different embolic materials. (A) DSA images of the MSAH group, (B) DSA images of the Gelfoam group, and (C) DSA images of the Coil group.

group, Gelfoam group, and Coil group, but the left IIA showed contrast agent overflow on DSA after the hemorrhage model was constructed. The bilateral IIA and its branches were not shown on DSA after embolization with the MSAH, and DSA taken 1 month later showed clear visualization of the bilateral IIA and its branches (Figure 5A). The bilateral IIA and its branches were not developed on DSA after embolization with the gelfoam particles, and DSA taken 1 month later showed no evidence of the bilateral IIA and its peripheral branches (Figure 5B). The bilateral IIA and its branches were not developed on DSA after embolization with the coil, and DSA taken 1 month later showed no evidence of the bilateral IIA and its peripheral branches (Figure 5C).

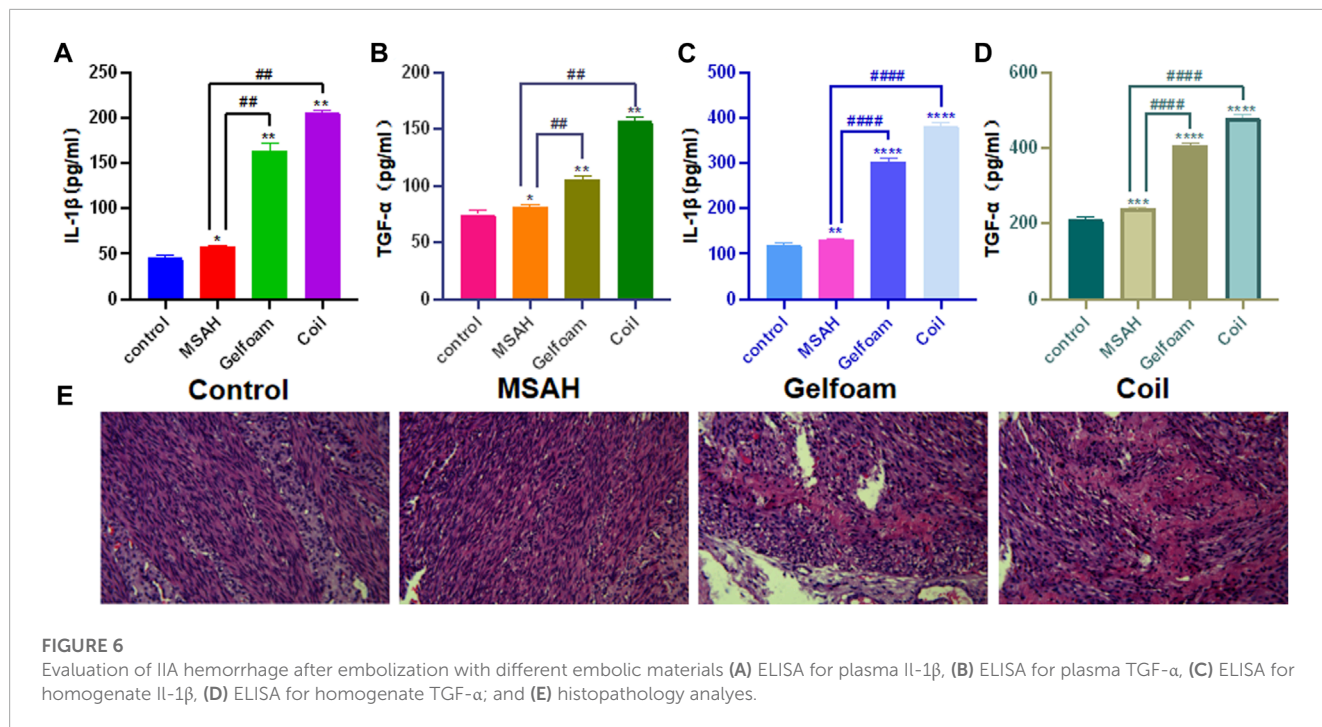
### Effects of different embolic materials on plasma inflammatory factors in the hemorrhage model

Blood was withdrawn from the ear vein 3 days after the operation. Plasma levels of TNF- $\alpha$  and IL-1 $\beta$  were detected using ELISA kits. The TNF- $\alpha$  levels were significantly higher in the MSAH group ( $p < 0.05$ ), in the GELFOAM group ( $p < 0.01$ ), and in the Coil group ( $p < 0.01$ ) compared to the Control group. Compared

with the MSAH group, the TGF- $\alpha$  levels were significantly higher in the Gelfoam group ( $p < 0.01$ ) and in the Coil group ( $p < 0.01$ ) (Figure 6A). Compared with the Control group, the plasma levels of IL-1 $\beta$  were significantly higher in the Gelfoam group ( $p < 0.01$ ) and in the Coil group ( $p < 0.01$ ), but not in the MSAH group ( $p > 0.05$ ). The plasma levels of IL-1 $\beta$  were significantly increased in the Gelfoam group ( $p < 0.01$ ) and the Coil group ( $p < 0.01$ ) compared to the MSAH group (Figure 6B).

### Changes in inflammatory factors in the uterine tissues after embolization in the hemorrhage model

The uterine homogenate supernatant was obtained 3 days after the second operation in the Control group and after bilateral IIA embolization in the MSAH group, Gelfoam group, and Coil group. Compared with the Control group, the TGF- $\alpha$  levels in the MSAH group ( $p < 0.01$ ) and the Gelfoam group ( $p < 0.01$ ) were significantly increased. Compared with the Control group, the TGF- $\alpha$  level in the Coil group was significantly increased ( $p < 0.01$ ). The TGF- $\alpha$  levels in the Gelfoam group were significantly increased compared with the MSAH group ( $p < 0.01$ ). The TGF- $\alpha$  levels were significantly



higher in the Coil group compared to the MSAH group ( $p < 0.01$ ) (Figure 6C). Compared with the blank control group, the IL-1 $\beta$  levels were significantly higher in the MSAH group ( $p < 0.01$ ), in the Gelfoam group ( $p < 0.01$ ), and in the Coil group ( $p < 0.01$ ). The IL-1 $\beta$  levels in the Gelfoam group were significantly higher than that in the MSAH group ( $p < 0.01$ ), and the IL-1 $\beta$  levels in the coil group were significantly higher than that in the MSAH group ( $p < 0.01$ ) (Figure 6D).

## Effect of different embolic materials on myometrium histopathology in a model of bleeding

Uterine pathology showed no lytic necrotic smooth muscle cells in the myometrium in the Control group. There were no necrotic smooth muscle cells in the myometrium in the MSAH group. There were moderate amounts of necrotic smooth muscle cells in the myometrium in the Gelfoam group. There was a large number of lytic and necrotic smooth muscle cells in the myometrium in the Coil group (Figure 6E).

## Discussion

In this study, SA was dissolved in ethanol, dispersed by magnetic stirring, and then mixed with NAO4 in different proportions for oxidation. Using this method, the oxidation effect was relatively satisfactory when the ratio of NAO4/SA was 1. The alginate was oxidized by NAO4 twice during the oxidation process, and the carbon-carbon bond of the alginate chain was destroyed after each oxidation, resulting in two aldehydes. The aldehydes increase the number of active functional groups of alginates, which makes

alginate biodegradable. This study provides a theoretical basis for the application of MSAH as a degradable vascular embolic material. In addition, the swelling rate and degradation rate of alginate can be adjusted by changing the oxidation degree (OD) of OSA. It has been reported that OSA, which has higher OD values, has a higher water absorption rate and higher degradation rate (Cai K et al., 2007). The biodegradable properties of alginate provide a new choice for biological tissue materials.

OSA powder was dissolved in purified water to prepare the OSA aqueous solution at 100 mg/mL, and CMC was dissolved in purified water to prepare the CMC aqueous solution at 30 mg/mL. The Schiff base reaction between the aldehyde group of OSA and the amino group of CMC is a mild chemical covalent cross-linking reaction, which does not require special and difficult reaction conditions. The Schiff base reaction is also a rapid reaction to ensure the speed of gelation. The rapid gelation of the MSAH provides a theoretical basis for its function as a vascular embolization material. In addition, when kept at 38°C for a longer time, the MSAH is more stable, adhesive, and hard, but the injectability worsens. Therefore, it is necessary to find an optimal water bath time to ensure the injectability of the modified alginate hydrogel with certain adhesion and hardness. Here, we found that the MSAH not only adhered to the wall of the silica gel tube but also had a certain hardness when the hydrogel was incubated in the water bath for 8 min. In addition, the hydrogel was successfully injected into the silica gel tube using a 1-mL syringe through a microcatheter.

It has been reported that Cynomolgus monkeys, pigs, dogs, rabbits, and mice can be used to establish a hemorrhage model. Although pigs, monkeys, and dogs have advantages, including large body size, thick blood vessels, and relatively easy intravascular intervention, they also have some disadvantages such as high cost and high demand for feeding site and conditions. Mice are

less costly and the feeding condition is simple, but the size of the mouse is too small and the blood vessels are thin, resulting in extreme difficulty of intravascular interventional procedures. The rabbit model of pelvic hemorrhage established in this study has been used in basic research to investigate the efficacy of interventional embolic materials. New Zealand rabbits are medium in size, and the vessel diameter is suitable for intravascular interventional procedures. In addition, the rabbits are not too costly and the feeding conditions are not demanding (Gao et al., 2008; Zhu et al., 2009; Chi Keung et al., 2014; Chang et al., 2018; Yu and Yi, 2019; Huang et al., 2021). Furthermore, the CIA of New Zealand rabbits is divided into the bilateral IIA and EIA, and the UA originates from the IIA, which is similar in humans (Liu et al., 2020). In this study, we found that the shape and anatomy of the arteries in the New Zealand rabbits nicely paralleled human anatomy.

Ideal bleeding embolism should achieve rapid hemostasis, without long-term necrosis of organs and tissues. At present, the commonly used materials for intravascular embolization are gelatin sponge particles, polyvinyl alcohol microspheres, and metal coils. Traditional particulate embolic agents are small in diameter, but can easily embolize the ends of blood vessels, resulting in ischemia and necrosis of normal tissues and organs. The metal spring embolic agent has a larger diameter but cannot be degraded and can easily cause permanent damage to blood vessels. Some studies have found that SA has the properties of swelling, biocompatibility, adhesion, and biodegradability. However, there are some disadvantages of using alginate alone as the embolic material, including weak mechanical properties of the gel, fragile gel structure in physiological saline, poor adhesion of the gel, and ease of embolizing vascular terminals due to its small particle diameter. In this study, the MSAH was prepared by oxidizing SA and then mixing it with a CMC aqueous solution at a certain proportion. This modification not only has the advantages of SA, such as biocompatibility, non-toxicity, and degradability, but also has new characteristics of high strength, strong viscosity, and embolization of the main arteries of bleeding vessels without influence on the vascular ends.

In this study, the MSAH was used to embolize the bilateral IIA in a New Zealand rabbit hemorrhage model. The modified alginate hydrogel resulted in the development of both sides of IIA and peripheral arteries, suggesting the long-term degradability of the modified alginate hydrogel. One month after embolization, the myometrium had almost no lysis and necrosis of myometrial smooth muscle cells, suggesting that the MSAH did not affect the blood flow of peripheral blood vessels and did not cause tissue ischemia and necrosis. It has been reported (Prieto-Moure et al., 2017; Xu et al., 2017) that tissue cells produce and release TNF- $\alpha$  after tissue ischemia to activate T cells, promote the production and secretion of IL-1 $\beta$ , and induce inflammation. In this study, we found that the levels of TNF- $\alpha$  and IL-1 $\beta$  both in the plasma and uterine tissue were significantly lower in the MSAH group than in the Gelfoam group and the Coil group, suggesting that MSAH can induce a slight inflammatory reaction and does not cause the peripheral tissue necrosis.

Altun et al. combined platelet rich fibrin fraction, nanoclay, and ethiodized oil to prepare a novel embolic biomaterial, blood-derived embolic materials (BEM). However, the disadvantages of

BEM are that it is a permanent embolism, which can easily lead to ischemic necrosis of organs and tissues (Altun et al., 2020). Rong et al. prepared a new biodegradable macromolecule material (thrombin-loaded alginate-calcium microspheres (TACMs), which is capable of hemostasis in a rabbit model of renal hemorrhage. TACMs are biodegradable, but due to their small diameter, they can easily embolize the peripheral blood vessels and cause tissue necrosis (Rong et al., 2015).

Through this study, we found that, on the one hand, MSAH can quickly embolize bleeding vessels with its strong viscosity and high intensity, but on the other hand, MSAH is characterized by good biocompatibility and degradability. After embolization of the bleeding vessels, we observed a mild inflammatory reaction is and no necrosis of the peripheral tissues. Thus, MSAH could potentially be used in the treatment of varying bleeding diseases, such as postpartum hemorrhage, acute gastrointestinal bleeding, traumatic rupture of parenchymal organs, bronchial artery hemorrhage, and tumor hemorrhage.

## Conclusion

In summary, MSAH not only has the same advantages of an alginate hydrogel such as biocompatibility, non-toxicity, and degradability, but also possesses new characteristics such as high strength and strong viscosity. In addition, the material can quickly embolize the main artery to stop bleeding in the early stage but does not embolize the peripheral branches of the bleeding artery to cause organ necrosis. Furthermore, the material can be degraded in the medium- and long-term without affecting the blood supply to the organs. This MSAH could be a new embolic material for clinical application.

## Data availability statement

The original contributions presented in the study are included in the article/supplementary material, further inquiries can be directed to the corresponding authors.

## Ethics statement

The animal study was approved by Animal Experimental Ethics Committee of Hainan Medical University. The study was conducted in accordance with the local legislation and institutional requirements.

## Author contributions

SW: Conceptualization, Data curation, Methodology, Writing—original draft. TD: Conceptualization, Methodology, Writing—review and editing. CW: Data curation, Writing—original draft. JS: Conceptualization, Writing—original draft. YL: Data curation, Writing—original draft. LH: Conceptualization, Writing—original draft. YL: Data curation, Writing—original draft. SZ: Conceptualization, Data curation, Writing—original draft. XJ: Conceptualization, Methodology, Writing—review and editing. GJ:

Conceptualization, Funding acquisition, Methodology, Resources, Validation, Writing–review and editing.

## Funding

The author(s) declare financial support was received for the research, authorship, and/or publication of this article. Natural Science Foundation of Hainan Province (820RC764, 823MS146), 2023 Provincial College Student Innovation and Entrepreneurship Training Program (S202311810051), Hainan Provincial Health Commission Scientific Research Project (22A200032), National College Students Innovation and Entrepreneurship Training Program (202211810017), Hainan Key Research and Development Social Development Project (ZDYF2022SHFZ293), and Hainan Province Clinical Medical Center (2021).

## References

- Altun, I., Hu, J., Albadawi, H., Zhang, Z., Salomao, M. A., Mayer, J. L., et al. (2020). Blood-derived biomaterial for catheter-directed arterial embolization. *Adv. Mater.* 32 (52), e2005603. doi:10.1002/adma.202005603
- Butwick, A., Lyell, D., and Goodnough, L. (2020). How do I manage severe postpartum hemorrhage? *Transfusion* 60 (5), 897–907. doi:10.1111/trf.15794
- Cai, K., Zhang, J., Deng, L., Yang, L., Hu, Y., Chen, C., et al. (2007). Physical and biological properties of a novel hydrogel composite based on oxidized alginate, gelatin and tricalcium phosphate for bone tissue engineering. *Adv. Eng. Mater.* 9 (12), 1082–1088. doi:10.1002/adem.200700222
- Cappell, M. S., and Friedel, D. (2008). Initial management of acute upper gastrointestinal bleeding: from initial evaluation up to gastrointestinal endoscopy. *Med. Clin. North Am.* 92 (3), 491–509. doi:10.1016/j.mcna.2008.01.005
- Chang, P., Cui, Y., and Xuemei, J. (2018). Application of ultrasound guidance in the establishment of rabbit model of knee joint hemorrhage. *Chin. J. Integr. Traditional West. Med.* 16 (5), 465–467.
- Chen, P., Xia, C., Mo, J., Mei, S., Lin, X., and Fan, S. (2018). Interpenetrating polymer network scaffold of sodium hyaluronate and sodium alginate combined with berberine for osteochondral defect regeneration. *Mater. Sci. Eng. C Mater. Biol. Appl.* 91, 190–200. doi:10.1016/j.msec.2018.05.034
- Chen, W., Lv, H., Liu, S., Liu, B., Zhu, Y., Chen, X., et al. (2017). National incidence of traumatic fractures in China: a retrospective survey of 512 187 individuals. *Lancet Glob. Health* 5 (8), e807–e817. doi:10.1016/s2214-109x(17)30222-x
- Chi Keung, T., Leung, M., and Ryoo, R. (2014). Application of minimally invasive balloon occlusion combined with surgical suture in the treatment of hemorrhagic renal injury in dogs. *PLA Med. J.* 26 (1), 10–12.
- Cothren, C. C., Osborn, P. M., Moore, E. E., Morgan, S. J., Johnson, J. L., and Smith, W. R. (2007). Preperitoneal pelvic packing for hemodynamically unstable pelvic fractures: a paradigm shift. *J. Trauma* 62 (4), 834–842. doi:10.1097/TA.0b013e31803c7632
- Gao, C., Chen, H., and Xiangzhen, L. (2008). Rat subarachnoid hemorrhage model was made by three methods. *Chin. J. Minim. Invasive Neurosurg.* 13 (9), 409–411.
- Huang, Y., Wu, S., and Xianghui, C. (2021). Establishment of a model of iliac artery rupture and bleeding under ultrasound guidance. *Chin. J. Ultrasound* 18 (4), 407–411.
- Liu, X., and Lei, H. (2020). Prevention and management of postpartum hemorrhage. *Chin. J. Pract. Gynecol. Obstet.* 36 (02), 123–126. doi:10.19538/j.fk2020020109
- Liu, X., Wang, Y., Liang, Z., Lian, X., Huang, D., Hu, Y., et al. (2023). Progress in preparation and application of sodium alginate microspheres. *Sheng Wu Yi Xue Gong Cheng Xue Za Zhi* 40 (4), 792–798. doi:10.7507/1001-5515.202211048
- Liu, Y., Zhang, Y., Ding, Y., Li, J., Tang, Q., Zhang, X., et al. (2020). Successful orthotopic uterine allotransplantation in a rabbit model using aorta and cava anastomoses: a short-term viability study. *Arch. Gynecol. Obstet.* 301 (2), 533–544. doi:10.1007/s00404-019-05381-9
- Majeed, A., Hwang, H. G., Eikelboom, J. W., Connolly, S., Wallentin, L., Feuring, M., et al. (2016). Effectiveness and outcome of management strategies for dabigatran- or warfarin-related major bleeding events. *Thromb. Res.* 140, 81–88. doi:10.1016/j.thromres.2016.02.005
- Park, H., and Lee, K. Y. (2014). Cartilage regeneration using biodegradable oxidized alginate/hyaluronate hydrogels. *J. Biomed. Mater. Res. A* 102 (12), 4519–4525. doi:10.1002/jbm.a.35126
- Prieto-Moure, B., Lloris-Carsí, J. M., Belda-Antolí, M., Toledo-Pereyra, L. H., and Cejalvo-Lapeña, D. (2017). Allopurinol protective effect of renal ischemia by downregulating TNF- $\alpha$ , IL-1 $\beta$ , and IL-6 response. *J. Invest. Surg.* 30 (3), 143–151. doi:10.1080/08941939.2016.1230658
- Rong, J. J., Liang, M., Xuan, F. Q., Sun, J. Y., Zhao, L. J., Zhen, H. Z., et al. (2015). Alginate-calcium microsphere loaded with thrombin: a new composite biomaterial for hemostatic embolization. *Int. J. Biol. Macromol.* 75, 479–488. doi:10.1016/j.ijbiomac.2014.12.043
- Tada, D., Tanabe, T., Tachibana, A., and Yamauchi, K. (2007). Recognition of four structurally resembled benzoic acid derivatives by albumin-crosslinked poly(acrylamide) hydrogel. *Mater. Sci. Eng. C, Biomim. Supramol. Syst.* C27 (4), 895–897. doi:10.1016/j.msec.2006.10.009
- Wu, Z., Li, Q., Xie, S., Shan, X., and Cai, Z. (2020). *In vitro* and *in vivo* biocompatibility evaluation of a 3D bioprinted gelatin-sodium alginate/rat Schwann-cell scaffold. *Mater. Sci. Eng. C Mater. Biol. Appl.* 109 (12), 110530. doi:10.1016/j.msec.2019.110530
- Xu, B., Hu, Q. H., Zhao, B., and Zhou, Z. K. (2017). Variation and significance of serum leptin, blood lipid level, adiponectin, NO and TNF- $\alpha$  for patients with non-traumatic ischemic necrosis of the femoral head. *Saudi J. Biol. Sci.* 24 (8), 1763–1766. doi:10.1016/j.sjbs.2017.11.008
- Yashaswini, D. G. V., Prabhu, A., Anil, S., and Venkatesan, J. (2021). Preparation and characterization of dexamethasone loaded sodium alginate-graphene oxide microspheres for bone tissue engineering. *J. Drug Deliv. Sci. Technol.* 64, 102624. doi:10.1016/j.jddst.2021.102624
- Yu, J., and Yi, Z. (2019). Outline of traumatic hemorrhage model in swine. *J. Northwest Def. Med.* 40 (3), 144–148.
- Yu, Z., Wang-Ping, D., Jian-Gong, L. U., and Orthopedics, D. O. (2016). *In vivo* and *in vitro* degradation of calcium alginate beads combined with chondrocytes. *Orthop. J. China* 24 (12), 1101–1106.
- Zaidi, A., Kohli, R., Daru, J., Estcourt, L., Khan, K. S., Thangaratinam, S., et al. (2020). Early use of fibrinogen replacement therapy in postpartum hemorrhage-A systematic review. *Transfus. Med. Rev.* 34 (2), 101–107. doi:10.1016/j.tmr.2019.12.002
- Zhu, H., Qin, L., and Minghua, F. (2009). Establishment and evaluation of Cynomolgus monkey cerebral hemorrhage model. *Chin. J. Comp. Med.* 19 (7), 29–32.

## Conflict of interest

The authors declare that the research was conducted in the absence of any commercial or financial relationships that could be construed as a potential conflict of interest.

## Publisher's note

All claims expressed in this article are solely those of the authors and do not necessarily represent those of their affiliated organizations, or those of the publisher, the editors and the reviewers. Any product that may be evaluated in this article, or claim that may be made by its manufacturer, is not guaranteed or endorsed by the publisher.